https://doi.org/10.1093/brain/awad301 BRAIN 2024: 147; 311–324 | 311

BRAIN
ORIGINAL ARTICLE

TRAPPC6B biallelic variants cause a neurodevelopmental disorder with TRAPP II and trafficking disruptions

Hashem Almousa,[1,†] Sara A. Lewis,[2,3,†] Somayeh Bakhtiari,[2,3] Sandra Hinz Nordlie,[2,3] Alex Pagnozzi,[4] Helen Magee,[2,3] Stephanie Efthymiou,[5] Jennifer A. Heim,[2] Patricia Cornejo,[6,7,8] Maha S. Zaki,[9,10] Najwa Anwar,[11] Shazia Maqbool,[11] Fatima Rahman,[11] Derek E. Neilson,[12] Anusha Vemuri,[13] Sheng Chih Jin,[14] Xiao-Ru Yang,[15] Abolfazl Heidari,[16] Koen van Gassen,[17] Aurélien Trimouille,[18] Christel Thauvin-Robinet,[19,20,21] James Liu,[2,3] Ange-Line Bruel,[20,21] Hoda Tomoum,[22] Mennatallah O. Shata,[22] Mais O. Hashem,[23] Mehran Beiraghi Toosi,[24,25] Ehsan Ghayoor Karimiani,[26] Gözde Yeşil,[27] Lokesh Lingappa,[28] Debangana Baruah,[28] Farnoosh Ebrahimzadeh,[29] Julien Van-Gils,[17] Laurence Faivre,[19] Mina Zamani,[30,31] Hamid Galehdari,[30] Saeid Sadeghian,[32] Gholamreza Shariati,[31,33] Rahema Mohammad,[5] Jasper van der Smagt,[17] Alya Qari,[34] John B. Vincent,[35] A. Micheil Innes,[15] Ali Dursun,[36] R. Köksal Özgül,[36] Halil Tuna Akar,[36] Kaya Bilguvar,[37,38] Cyril Mignot,[39,40] Boris Keren,[39] Claudia Raveli,[41] Lydie Burglen,[42] Alexandra Afenjar,[42] Laura Donker Kaat,[43] Marjon van Slegtenhorst,[43] Fowzan Alkuraya,[23] Henry Houlden,[5] Sergio Padilla-Lopez,[2,3] Reza Maroofian,[5,‡] Michael Sacher[1,44,‡] and Michael C. Kruer[2,3,‡]

[†,‡]These authors contributed equally to this work.

Highly conserved transport protein particle (TRAPP) complexes regulate subcellular trafficking pathways. Accurate protein trafficking has been increasingly recognized to be critically important for normal development, particularly in the nervous system. Variants in most TRAPP complex subunits have been found to lead to neurodevelopmental disorders with diverse but overlapping phenotypes. We expand on limited prior reports on *TRAPPC6B* with detailed clinical and neuroradiologic assessments, and studies on mechanisms of disease, and new types of variants.

We describe 29 additional patients from 18 independent families with biallelic variants in *TRAPPC6B*. We identified seven homozygous nonsense ($n = 12$ patients) and eight canonical splice-site variants ($n = 17$ patients). In addition, we identified one patient with compound heterozygous splice-site/missense variants with a milder phenotype and one patient with homozygous missense variants.

Patients displayed non-progressive microcephaly, global developmental delay/intellectual disability, epilepsy and absent expressive language. Movement disorders including stereotypies, spasticity and dystonia were also observed. Brain imaging revealed reductions in cortex, cerebellum and corpus callosum size with frequent white matter hyperintensity. Volumetric measurements indicated globally diminished volume rather than specific regional losses.

We identified a reduced rate of trafficking into the Golgi apparatus and Golgi fragmentation in patient-derived fibroblasts that was rescued by wild-type TRAPPC6B. Molecular studies revealed a weakened interaction between mutant TRAPPC6B (c.454C>T, p.Q152*) and its TRAPP binding partner TRAPPC3. Patient-derived fibroblasts from the

Received April 18, 2023. Revised July 11, 2023. Accepted August 10, 2023. Advance access publication September 15, 2023

TRAPPC6B (c.454C>T, p.Q152*) variant displayed reduced levels of TRAPPC6B as well as other TRAPP II complex-specific members (TRAPPC9 and TRAPPC10). Interestingly, the levels of the TRAPPC6B homologue TRAPPC6A were found to be elevated. Moreover, co-immunoprecipitation experiments showed that TRAPPC6A co-precipitates equally with TRAPP II and TRAPP III, while TRAPPC6B co-precipitates significantly more with TRAPP II, suggesting enrichment of the protein in the TRAPP II complex. This implies that variants in *TRAPPC6B* may preferentially affect TRAPP II functions compared to TRAPP III functions. Finally, we assessed phenotypes in a *Drosophila TRAPPC6B*-deficiency model. Neuronal TRAPPC6B knockdown impaired locomotion and led to wing posture defects, supporting a role for TRAPPC6B in neuromotor function.

Our findings confirm the association of damaging biallelic *TRAPPC6B* variants with microcephaly, intellectual disability, language impairments, and epilepsy. A subset of patients also exhibited dystonia and/or spasticity with impaired ambulation. These features overlap with disorders arising from pathogenic variants in other TRAPP subunits, particularly components of the TRAPP II complex. These findings suggest that TRAPPC6B is essential for brain development and function, and TRAPP II complex activity may be particularly relevant for mediating this function.

1 Department of Biology, Concordia University, Montreal, Quebec H4B1R6, Canada
2 Barrow Neurological Institute, Phoenix Children's Hospital, Phoenix, AZ 85016, USA
3 Departments of Child Health, Cellular and Molecular Medicine, Genetics, and Neurology, University of Arizona College of Medicine—Phoenix, Phoenix, AZ 85004, USA
4 CSIRO Health and Biosecurity, The Australian e-Health Research Centre, Brisbane 4029, Australia
5 Department of Neuromuscular Disorders, UCL Queen Square Institute of Neurology, London WC1N 3BG, UK
6 Pediatric Neuroradiology Division, Pediatric Radiology, Barrow Neurological Institute, Phoenix Children's Hospital, Phoenix, AZ 85016, USA
7 Department of Child Health, University of Arizona College of Medicine, Phoenix, AZ 85004, USA
8 Department of Radiology, Mayo Clinic, Scottsdale, AZ 85259, USA
9 Clinical Genetics Department, Human Genetics and Genome Research Division, National Research Centre, Cairo 12622, Egypt
10 Genetics Department, Armed Forces College of Medicine (AFCM), Cairo 4460015, Egypt
11 Department of Developmental-Behavioural Paediatrics, The Children's Hospital and Institute of Child Health, Lahore 54000, Pakistan
12 Genetics and Metabolism, Phoenix Children's Hospital, Phoenix, AZ 85016, USA
13 Department of Pathology, University of Chicago, Chicago, IL 60637, USA
14 Department of Genetics, Washington University, St.Louis, MO 63110, USA
15 Department of Medical Genetics and Alberta Children's Hospital Research Institute, Cumming School of Medicine, University of Calgary, S.W. Calgary, AB T2N 4N1, Canada
16 Reference Laboratory, Qazvin Medical University, Qazvin 34148-33245, Iran
17 Division of Laboratories, Pharmacy and Biomedical Genetics, Section of Clinical Genetics, University Medical Center Utrecht (UMCU), 3584 CX Utrecht, Netherlands
18 Laboratoire de Génétique Moléculaire, Service de Génétique Médicale, CHU Bordeaux—Hôpital Pellegrin, Place Amélie Raba Léon, 33000 Bordeaux, France
19 Department of Genetics and Reference Center for Development Disorders and Intellectual Disabilities, FHU TRANSLAD, CHU Dijon Bourgogne, 21000 Dijon, France
20 Unité Fontctionnelle d'Innovation diagnostiques des maladies rares, FHU TRANSLAD, CHU Dijon Bourgogne, 21000 Dijon, France
21 GAD 'Génétique des Anomalies du Développement', INSERM-Université de Bourgogne UMR1231, 21078 Dijon, France
22 Department of Pediatrics, Ain Shams University, Cairo 11516, Egypt
23 Department of Translational Genomics, Center for Genomic Medicine, King Faisal Specialist Hospital and Research Centre, Riyadh 11211, Saudi Arabia
24 Pediatric Neurology Department, Ghaem Hospital, Mashhad University of Medical Sciences, Mashhad 13944-91388, Iran
25 Neuroscience Research Center, Mashhad University of Medical Science, Mashhad 13944-91388, Iran
26 Molecular and Clinical Sciences Institute, St.George's, University of London, London SW17 0RE, UK
27 Istanbul Medical Faculty Department of Medical Genetics, Istanbul University, Istanbul 34452, Turkey
28 Pediatric Neurology, Rainbow Children Hospital, Hyderabad 500034, India
29 Department of Internal Medicine, Mashhad University of Medical Sciences, Mashhad 13944-91388, Iran
30 Department of Biology, Faculty of Science, Shahid Chamran University of Ahvaz, Ahvaz 6135783151, Iran
31 Narges Medical Genetics and Prenatal Diagnosis Laboratory, Ahvaz 6155889467, Iran
32 Department of Pediatric Neurology, Golestan Medical, Educational, and Research Center, Ahvaz Jundishapur University of Medical Sciences, Ahvaz 6135733118, Iran

33 Department of Medical Genetics, Faculty of Medicine, Ahvaz Jundishapur University of Medical Sciences, Ahvaz 6135733118, Iran
34 Medical Genomics Department, Center for Genomic Medicine, King Faisal Specialist Hospital and Research Center, Riyadh 11564, Saudi Arabia
35 Molecular Neuropsychiatry & Development (MiND) Lab, Campbell Family Mental Health Research Institute, Centre for Addiction and Mental Health, Toronto, ON M6J 1H4, Canada
36 Department of Pediatric Metabolism, Hacettepe University, Faculty of Medicine & Institute of Child Health, Ankara 06800, Turkey
37 Department of Medical Genetics, Acibadem Mehmet Ali Aydinlar University, Istanbul 34752, Turkey
38 Department of Neurosurgery and Genetics, Yale University School of Medicine, New Haven, CT 06520, USA
39 Département de Génétique, APHP Sorbonne Université, Hôpital Trousseau & Groupe Hospitalier Pitié-Salpêtrière, 75013 Paris, France
40 Centre de Référence Déficiences Intellectuelles de Causes Rares, 75012 Paris, France
41 APHP Sorbonne Université, Service de Neuropédiatrie, Hôpital Trousseau, 75012 Paris, France
42 Département de Génétique, Centre de référence des malformations et maladies congénitales du cervelet, APHP. Sorbonne Université, Hôpital Trousseau, 75012 Paris, France
43 Department of Clinical Genetics, Erasmus Medical Center, 3000 Rotterdam, The Netherlands
44 Department of Anatomy and Cell Biology, McGill University, Montreal, Quebec H3A0C7, Canada

Correspondence to: Michael Kruer
Departments of Child Health, Neurology, and
Cellular & Molecular Medicine and Program in Genetics
University of Arizona College of Medicine—Phoenix
Arizona Biomedical Collaborative Building – 1, Phoenix, AZ 85004, USA
E-mail: kruerm@arizona.edu

Keywords: TRAPPC6B; NEDMEBA; TRAPPopathy; TRAPP-II complex; ER-golgi trafficking; Trs33

Introduction

Trafficking protein particle (TRAPP) complexes regulate vesicle trafficking via guanine nucleotide exchange factor (GEF) activity of Rab GTPases[1] and localization to compartments such as the Golgi apparatus.[2] Two TRAPP complexes have been identified in mammals called TRAPP II and TRAPP III. While both complexes activate Rab1 *in vitro*,[2] TRAPP II additionally activates Rab11,[2,3] a GTPase that also functions in ciliogenesis.[4] TRAPP II proteins have also been implicated in ciliogenesis.[5] On the other hand, TRAPP III has been implicated in early secretory pathway traffic and autophagy.[6,7] Knockdowns and mutations in both TRAPP II- and III-specific proteins have been shown to affect trafficking into and through the Golgi as well as affecting Golgi morphology.[8] TRAPP-mediated trafficking is crucial for brain development and function, as variants in multiple TRAPP subunits lead to overlapping neurodevelopmental disorders, with movement disorders, intellectual disability, epilepsy and neuromuscular features (Table 1).[8]

Both TRAPP complexes are built upon a common catalytic core of proteins that include TRAPPC1, TRAPPC2, TRAPPC2L, TRAPPC3, TRAPPC4, TRAPPC5 and TRAPPC6. For the TRAPP II complex, TRAPPC9 and TRAPPC10 are linked to the core while the TRAPP III complex contains the core with TRAPPC8, TRAPPC11 and TRAPPC12.[6,22,23] Two genes encoding the core TRAPPC6 protein have been reported in humans called *TRAPPC6A* and *TRAPPC6B*.[24] *Drosophila melanogaster* and *Saccharomyces cerevisiae* have a single gene encoding this subunit, *Trs33*. It has been assumed that TRAPPC6A and TRAPPC6B could incorporate into either TRAPP II or TRAPP III complex, as both proteins are capable of forming a heterodimer in complex with TRAPPC3 *in vitro*.[24-26]

A homozygous nonsense variant in *TRAPPC6B* was recently described in an Iranian family in association with intellectual disability[27] and a homozygous splice-site founder mutation was found in three Egyptian families in association with microcephaly, intellectual disability, autism, epilepsy, dystonia and reduced brain volume.[9] A fifth family was then reported.[28] In this report, we describe 29 individuals from 18 unrelated families with biallelic variants in *TRAPPC6B* manifesting microcephaly, epilepsy and intellectual disability with phenotypic expansion to include spasticity. We examine variant impact on TRAPPC6B and TRAPP II- versus TRAPP III-specific protein levels, anterograde protein trafficking, and Golgi apparatus morphology in patient fibroblasts. Finally, we tested whether *TRAPPC6B* can regulate neuromotor function using *Drosophila* locomotor and wing posture assays. Together, the findings expand the *TRAPPC6B*-associated clinical and neuroradiologic phenotype and demonstrate patient variants disrupt TRAPPC6B and TRAPP II protein levels, trafficking and Golgi morphology. We further find that TRAPPC6B preferentially associates with TRAPP II complex members, which support the observation that TRAPPC6B clinical phenotypes more closely align with TRAPP II complex disorders.

Materials and methods

Patient recruitment, sequencing and variant calling

All human subject studies were performed in accordance with the ethical standards of the responsible committee on human experimentation according to institutional and national standards. Proper informed consent was obtained for all participants. Clinical phenotypes (Supplementary material) were abstracted from written records, supplemented by review of available neuroimaging, facial photographs and laboratory and clinical electrophysiologic data. Patient videos were reviewed by paediatric movement disorder neurologists (J.H. and M.C.K.). Phenograms

Table 1 TRAPP genes with neurological disease connections

Gene (OMIM#/*), citation	Complex	Disease	Cognitive findings	Epilepsy	Movement disorder	White matter	Brain volume	Language	Dysmorphic features	Visual system	Muscle findings
TRAPPC6B (#617862),[9] this study	II, III	NEDMEBA	ID	Variable	Spasticity, dystonia, stereotypies	Thin corpus callosum, hyperintensity	Brain volume loss, microcephaly	Absent expressive language	Variable	No impairments	Reduced bulk
TRAPPC2L (#618331)[10,11]	II, III	PEERB	ID	Focal seizures and status epilepticus with infection	Tetraplegia; dystonia	Normal-delayed myelination	Variable atrophy	Absent speech	NR	Cerebral visual impairment	Rhabdomyolysis; non-specific biopsy
TRAPPC4 (#618741)[12-14]	II, III	NEDESBA	Normal-severe ID; regression	Yes	Spasticity; axial hypotonia; variable dyskinesia	White matter loss	Mild-severe cerebral atrophy; secondary microcephaly	Delay and loss of expressive language	Yes	Visual impairments; variable cataracts	Amyotrophy
TRAPPC6A (*610396)[15]	II, III	NDD	ID	NR	NR	NR	NR	Speech delay	Yes	NR	NR
TRAPPC9 (#613192)[16,17]	II	MRT13	Moderate-severe ID	Variable seizures	Hypotonia, stereotypies	Thin corpus callosum, reduced white matter	Postnatal microcephaly	Speech disorder	Yes	NR	NR
TRAPPC10 (*602103)[18,19]	II	NDD	Severe ID	Variable seizures	Hypotonia, waddling gait	1 patient thin corpus callosum	Microcephaly	Poor speech	NR	Low frequency strabismus	NR
TRAPPC11 (#615356)[20]	III	LGMD	Normal-severe ID	Variable (generalized seizures)	Some with ataxia and/or choreiform movements	Some reduced volume	Normal-microcephaly; some cerebral atrophy	NR	NR	Variable (amblyopia, cataract)	LGMD
TRAPPC12 (#617669)[21]	III	PEBAS	Severe DD and regression	Seizures; myoclonus	Spasticity; truncal hypotonia; dystonia	Corpus callosum agenesis; hyper-intensity	Microcephaly; pons hypoplasia; diffuse atrophy	NR	NR	Optic atrophy; cortical visual impairment	NR

= phenotype MIM number; * = gene/locus MIM number. ID = intellectual disability; LGMD = limb girdle muscular dystrophy; MRT13 = mental retardation, autosomal recessive 13; NDD = neurodevelopmental disorder; NEDESBA = neurodevelopmental disorder with epilepsy, spasticity and brain atrophy; NEDMEBA = neurodevelopmental disorder with microcephaly, epilepsy and brain atrophy; NR = not reported; PEBAS = progressive encephalopathy with brain atrophy and spasticity; PEERB = progressive encephalopathy with episodic rhabdomyolysis.

were created using R (4.1.0). Patients with data not available for a category were not included in that category's calculations. TRAPP disease gene summary was created from OMIM.org, accessed August 2022. Sequencing details and filtering criteria used for each case are provided in the Supplementary material.

MRI analysis, processing and volumetric quantification

Neuroimaging findings were reviewed and summarized by a board-certified neuroradiologist (P.C.). Several image processing steps were then performed on the T1-weighted brain MRIs,[29] including registration to the Colin 27 Average Brain Atlas, correcting image bias using the N4 algorithm, followed by intensity normalization and image de-noising, using anisotropic diffusion. Skull stripping was performed using an in-house algorithm developed in Python. In this approach, intradural CSF was identified using thresholding and morphological operations, following which the lateral ventricles were isolated based on their spatial location, allowing the volume of the lateral ventricles (in ml) to be extracted. Cerebral brain tissues (grey matter, white matter) were then isolated based on their MR intensities using the Expectation Maximization (EM)/Markov Random Field (MRF) approach. From the cortical grey matter segmentation, three measures of cortical shape were performed (cortical thickness, curvature and sulcal depth) to quantify shape abnormalities. Measures were converted to a z-score from healthy cortical shape measures measured from the corresponding cortical region compared to the Child Mind Institute Healthy Brain Network cohort of 564 typically developing children (TDC) (Eq. 1), based on cortical regions from the Automated Anatomical Labelling (AAL) atlas.

$$z\text{-}score_{subject} = \frac{(x_{subject} - \mu_{TDC})}{\sigma_{TDC}} \quad (1)$$

MRI statistical analysis

Six participants passed the quality checks for initial MRI data quality and processed segmentations (Families 3, 4, 6 and 10). For each participant, z-scores of grey matter volume, white matter volume and ventricle asymmetry (Eq. 2), were extracted.

$$Ventricle\ asymmetry = \frac{(vol_{left} - vol_{right})}{(vol_{left} + vol_{right})} \quad (2)$$

Yeast two-hybrid assay

TRAPP open reading frames were cloned into pGADT7 and pGBKT7 plasmids (Clontech). Standard yeast methods were used for transformation of the pGADT7 and pGBKT7 constructs into AH109 and Y187 yeast strains, respectively. Diploid cells were produced by mating on solid YPD media and then selected for on solid synthetic complete (SC) media lacking leucine and tryptophan (DDO). Single colonies of each diploid were then cultured in liquid DDO and then spotted on either DDO or on SC media lacking leucine, tryptophan and histidine (TDO) to assess for interactions. Plates were grown at 30°C for 72 h.

Membrane trafficking assay

The retention using selective hooks (RUSH) assay was performed as described in Boncompain *et al.*[30] Briefly, fibroblasts grown in Dulbecco's modified Eagle medium (DMEM) supplemented with 10% fetal bovine serum were transfected by electroporation with the Golgi-resident enzyme sialyl transferase-GFP (ST-GFP) fused to streptavidin binding protein. The plasmid also expressed KDEL-tagged streptavidin for endoplasmic reticulum (ER) retention. For the rescue experiments, fibroblasts were co-transfected with ST-GFP and TRAPPC6B-RFP. Twenty-four hours after transfection, biotin was added to a final concentration of 60 μM to release the reporter from the ER hook. Live cells were imaged by florescence microscopy every 2 min for 60 min using a Nikon Livescan sweptfield confocal microscope with a 40× objective lens (NA 0.95). Integrated fluorescence intensity at the Golgi region and from whole cell was measured every 2 min using ImageJ v1.53. The ratio between fluorescent intensities within the Golgi and whole cell was generated for each time point. The first time point corresponding to background was subtracted from all time points. These values were then plotted as the mean percentage of maximal intensity.

Golgi morphology

Fibroblasts were cultured in DMEM supplemented with 10% fetal bovine serum. The cells were washed twice with PBS solution then fixed with 4% paraformaldehyde (PFA) for 15 min at room temperature, quenched with 0.1 M glycine for 10 min and permeabilized with 0.1% Triton X-100 for 7 min. Blocking was performed in 5% normal goat serum in PBS for 45 min at room temperature. Primary antibodies were prepared in 5% normal goat serum and were added to the cells and incubated overnight at 4°C. Cells were washed twice for 5 min each with PBS. Secondary antibodies were diluted in 5% normal goat serum in PBS and incubated with the cells at room temperature for 1 h and then removed. Hoechst 33342 (Thermo Fisher Scientific) was diluted in PBS (1:2000) and added to stain the nucleus for 2 min followed by two washes with PBS for 10 min each. The coverslips were then mounted with ProLong Gold Anti Fade. Images were acquired on an Olympus FV10i confocal laser scanning microscope fitted with a 60× objective (NA 1.35). The number of Golgi fragments per cell were quantified using Imaris software c.9.8.0 (Bitplane). Golgi structures were identified from the mannosidase II channel using the following surface parameters: surface details = 0.22 μm; and thresholding with a background subtraction of the depicted Golgi spherical structures that have diameter smaller than 0.55 μm in size. Statistical analyses were carried out using one-way ANOVA corrected for Tukey's multiple comparisons using GraphPad Prism 6.01. A *P*-value of 0.05 was considered to be statistically significant.

Immunoblotting

Fibroblasts were washed twice with PBS and lysed in a solution containing 50 mM Tris pH 7.2, 150 mM NaCl, 0.5 mM EDTA, 1 mM DTT, 1% Triton X-100 and protease inhibitor cocktail (EDTA-free; Roche). The lysate was clarified at 13 000*g* for 30 min at 4°C. A total of 30–40 μg of whole cell lysate was loaded and fractionated in either 8 or 15% SDS-polyacrylamide gels. The gels were transferred to nitrocellulose membranes and blocked with 5% skimmed milk powder in PBS with 0.1% Tween (PBS-T) for 1 h. Primary antibodies were incubated in PBS-T overnight at 4°C, washed three times with PBS-T for 5 min each, and secondary antibodies were incubated for 1 h at room temperature. Membranes were then washed three times with PBS-T for 5 min each and incubated with Pierce ECL western blot substrate (Thermo Fisher Scientific) and detected using an Amersham Imager 600 (GE Healthcare).

Immunoprecipitation

HeLa cells were seeded in 10 cm dishes 24 h prior to co-transfecting cells with 5 μg of DNA expressing either TRAPPC6A-V5/TRAPPC10-FLAG, TRAPPC6A-V5/TRAPPC11-FLAG, TRAPPC6B-V5/TRAPPC10-FLAG or TRAPPC6B-V5/TRAPPC11-FLAG using Jet Prime (Polyplus). Forty-eight hours after transfection, cells were washed twice with ice cold PBS and lysed in a solution containing 50 mM Tris pH 7.2, 150 mM NaCl, 0.5 mM EDTA, 1 mM DTT, 1% Triton X-100 and protease inhibitor cocktail (EDTA-free; Roche). The lysate was clarified at 13 000*g* for 30 min at 4°C. A total of 500 μg of lysate was incubated with 20 μl (10 μl bead volume) anti-Flag M2 affinity beads (Sigma Aldrich) in IP-buffer (50 mM Tris pH 7.2, 150 mM NaCl, 0.5 mM EDTA, 0.1% Triton X-100 and protease inhibitor cocktail) for 3 h at 4°C on an orbital shaker. The beads were collected by centrifugation at 5000 rpm for 30 s at 4°C and washed twice with IP-buffer and twice with IP-buffer without Triton X-100. The beads were resuspended in 20 μl of 2× Laemmli sample buffer containing β-mercaptoethanol and heated at 95°C for 5 min to dissociate the immune complexes. The beads were pelleted by centrifugation and SDS-PAGE for protein from input (whole-cell extracts) and immunoprecipitated proteins was performed as described above.

Molecular biology techniques

Standard molecular biological techniques were used to generate FLAG-tagged, RFP-tagged and V5 tagged constructs. TRAPPC6B variants were generated by site-directed mutagenesis.

Antibodies

Antibodies used in this study were: anti-TRAPPC2L (1:1000 mouse monoclonal, Santa Cruz sc-377322), anti-TRAPPC3 (1:1000 rabbit polyclonal[31]), anti-TRAPPC6A (1:500 mouse monoclonal, Santa Cruz sc-376032), anti-TRAPPC6B (1:1000 rabbit polyclonal, ABclonal A15561), anti-TRAPPC8 (1:1000 rabbit polyclonal, Abcam ab122692), anti-TRAPPC9 (1:2000 rabbit polyclonal, LS Bio LS-C750497), anti-TRAPPC10 (1:500 mouse monoclonal, Santa Cruz sc-101259), anti-TRAPPC12 (1:1000 rabbit polyclonal[31]), anti-FLAG (1:5000 mouse monoclonal, Sigma F1804), anti-α-Tubulin (1:5000 mouse monoclonal, Sigma T6199), anti-RFP (1:500 mouse monoclonal, Rockland 200-301-379S), anti-mannosidase II (1:200 kind gift from Dr Kelley Moreman) and anti V5 (1:1000 rabbit monoclonal, Cell Signaling 13202).

Fly rearing and genetics

Drosophila were reared on a standard cornmeal, yeast, sucrose food from the BIO5 media facility, University of Arizona. Stocks for experiments were reared at 25°C, 60–80% relative humidity, with a 12:12 light/dark cycle. Crosses for controls and mutants and animals selected for locomotor assay were maintained at an elevated temperature of 28.5°C. Fly stocks were obtained from the Bloomington Drosophila Stock Center (NIH P40OD018537). Crosses were performed with w^{1118} for heterozygous studies of genetic controls. P[TRiP.HMJ21139]attP40 was used for expression of UAS-Trs33-RNAi.[32] Pan-neuronal Gal4 driver (ELAV, CG4262) was used to direct RNAi expression to post-mitotic neurons during development and throughout adulthood.

Locomotor assays

Naïve, unmated flies collected as pharate adults and controlled for humidity, temperature and time of day (30% RH, 24°C, 09.00–11.00) were used. Flies at 14 days post-eclosion were adapted to room conditions for 1 h before assaying in groups of 3–20 in coded vials by blinded experimenters.[33] Distance was determined from still images from video at 3 s post-tapping using ImageJ measured distance function from the middle of the fly to the bottom of the vial and averaged between flies for each trial. Graphs and *t*-test statistic calculations were performed in R (4.1.0). For box and whisker plots, box indicates 75th and 25th percentile with median line; whiskers indicate range of data.

Erect wing scoring

Each video was manually assessed for flies with erect wing phenotype defined as wings held upright and away from the body.[34] The wing must have been held erect during the majority of the video, and upright wing postures limited to before flight or during grooming were excluded. Statistics were determined both three-way and pairwise against both control genotypes using chi-squared analysis in R (4.1.0).

Results

Through Genematcher, we identified 18 families with biallelic variants in *TRAPPC6B* from international collaborators. In our cohort, 27/29 individuals segregated loss-of-function (nonsense and splice-site) homozygous variants, with one individual carrying compound heterozygous splice-site/missense variants and one individual carrying homozygous missense variants. The male:female ratio was 1.6:1 and average age of diagnosis was 7.5 years (range 14 months to 35 years). Affected families were from 11 countries (Iran, Morocco, Pakistan, Tunisia, France, Mali, Gambia, Egypt, Saudi Arabia, Turkey and India) and frequently included multiple affected individuals (Supplementary Fig. 1). Homozygous variants, including seven homozygous nonsense ($n = 12$ individuals), eight canonical splice-site variants ($n = 17$ individuals) and one missense variant ($n = 1$ individual), were identified using whole-exome sequencing. Variant information is provided in Supplementary Table 1. Additional sequencing information is provided in the Supplementary material.

We conducted detailed clinical and neuroradiologic assessments. Frequency of clinical features are summarized in Table 2 and Fig. 1A with full descriptions in the Supplementary material. We noted a constellation of cognitive and motor features partially overlapping a prior report of individuals with *TRAPPC6B* variants.[9] Consistent with prior reports, we found complex neurodevelopmental features including intellectual disability, expressive language defects, autism, seizures or epilepsy, and neurobehavioural features such as aggression and self-injury in some patients (Fig. 1A). Many patients also exhibited difficulty with walking and some also had issues sitting. Stereotyped movements were evident in most individuals, with dystonia, spasticity and contractures at lower frequency. On examination, knee-jerk reflexes were often increased, although they were absent in one patient. Reduced muscle bulk was occasionally observed in the most impaired patients (Gross Motor Function Classification System 4–5). Microcephaly was a notable feature in this cohort, with some patients as severe as <−6.5 SD. This microcephaly does not appear to be progressive based on serial clinical assessments. Dysmorphic features include a variety of inconsistent facial features, tapered fingers, and arachnodactyly (Fig. 1B–N). MRI was assessed for 16 individuals (Fig. 2) and identified reductions in cortex and cerebellum with increased ventricle size. Foreshortening or thinning of corpus callosum and white matter increased intensity or volume loss were consistent imaging features. Volumetric measures of MRI compared to age-

Table 2 Clinical features of TRAPPC6B patients

Family	Patient	Walk	Sit	GMFCS	Verbal	Seiz.	Spast.	Contractures	Dystonia	Reflex	Muscle loss	Stereotypies	Microcephaly	Facial feat.[a]	Hand/ foot[b]	Other organ[c]	ID/ GDD	ASD	Behavioural[d]
1	1	++	++	5	+	+	+	+	+	–	+	+	Yes	+	0	0	+	0	0
	2	++	++	5	+	+	+	+	+	0	+	+	Yes	+	0	0	+	0	0
2	3	++	+	5	+	+	++	+	0	+	N/A	+	Yes, prog.	+	+	0	+	N/A	0
3	4	+	0	N/A	+	+	++	+	+	N/A	N/A	+	–3 SD 35 y	+	+	0	+	N/A	+
4	5	+	0	4	+	++	0	0	0	+	+	+	–6.5 SD 15 y	+	+	0	+	N/A	0
	6	++	+	5	+	0	0	+	0	+	+	+	–6 SD 11 y	+	+	+	+	N/A	0
5	7	0	0	3	+	0	0	0	0	0	N/A	+	No, –1.3 SD 3.5 y	+	0	+	+	0	+
6	8	0	0	2	+	0	0	0	0	0	N/A	+	–2.5 SD 5 y	+	+	+	+	0	0
7	9	0	0	N/A	+	0	+	0	0	0	+	+	–2 SD birth	+	0	0	+	N/A	0
8	10	+	0	N/A	+	+	Yes	0	0	+	N/A	+	–2 SD birth	+	+	0	+	+	+
9	11	0	0	N/A	+	0	0	0	0	0	N/A	+	–2 SD 4 y 4 m	0	0	+	+	+	+
	12	0	0	N/A	N/A	0	0	0	0	0	N/A	N/A	–2 SD	0	0	0	+	+	+
10	13	0	0	N/A	+	++	0	0	0	N/A	N/A	N/A	–5.2 SD 11 y	+	0	0	+	+	0
	14	0	0	N/A	+	0	0	0	0	N/A	N/A	N/A	–5.7 SD 6 y	0	0	0	+	+	0
	15	++	0	N/A	+	0	0	0	0	N/A	N/A	N/A	–2.4 SD 14 m	0	0	0	+	+	0
	16	0	0	N/A	+	0	0	0	0	N/A	N/A	N/A	N/A	0	0	0	+	0	0
11	17	++	0	N/A	+	0	Yes	+	0	0	N/A	+	N/A	0	0	0	+	N/A	0
	18	0	0	N/A	+	0	0	+	0	0	N/A	+	Yes	0	0	0	+	N/A	0
12	19	0	0	N/A	+	++	Yes	0	0	0	N/A	N/A	Yes	0	0	0	+	+	0
	20	+	0	N/A	+	0	0	0	0	0	N/A	0	Yes	0	0	0	+	N/A	0
13	21	++	0	4	N/A	++	++	N/A	0	N/A	N/A	+	2 SD birth	+	+	0	+	+	0
14	22	0	0	N/A	N/A	++	Yes	+	0	+	N/A	+	–4.3 SD 5 y	0	0	0	+	+	0
15	23	0	0	N/A	+	0	0	0	0	+	N/A	+	No –1.4 SD	0	0	0	+	+	+
	24	0	0	N/A	+	0	0	0	0	+	N/A	0	No –0.5 SD	0	0	+	+	0	0
16	25	0	0	N/A	+	0	+	+	+	+	0	+	–4.8 SD	+	0	+	+	+	+
	26	0	0	N/A	+	0	+	+	+	+	0	+	–4.8 SD	+	0	+	+	+	+
17	27	0	0	N/A	+	++	+	N/A	0	N/A	0	0	–2.4SD 30 y	0	0	0	+	0	0
	28	0	0	N/A	+	++	+	N/A	0	N/A	0	0	–2.8 SD 30 y	0	0	0	+	0	0
18	29	+	0	4	+	++	+	0	0	+	N/A	0	Yes, 46 cm	0	0	0	+	0	0

+ = defects present; 0 = no abnormalities; ASD = autism spectrum disorder; feat. = features; GMFCS = Gross Motor Function Classification System; ID/GDD = seizure intellectual disability/global developmental delay; N/A = data not available; m = months; prog = progressive; SD = standard deviation; seiz. = seizure; sit = sitting ability; spast. = spasticity; walk = walking ability; y = years. Walking scores: 0 = walks unassisted, + = walks with assistance or gait impairment present, ++ = cannot walk; Sitting scores: 0 = sits without support, + = sits with support, ++ = cannot sit; Verbal scores: 0 = normal speech, + = impaired age-appropriate expressive language. Seizure scores: 0 = no seizures, + = only one seizure in medical history, ++ = epilepsy. Spasticity scores: 0 = none, + = lower limbs only, ++ = upper + lower body involvement. Dystonia scores: 0 = no, + = generalized affecting ≥2 limbs; Reflex scores: – = absent knee-jerk reflex, 0 = normal, + = exaggerated/brisk; Muscle loss scores: 0 = none, + = atrophy or reduced bulk with or without hypotonia; ASD scores: 0 = no, + = yes, N/A may also refer to inability to assess due to severity of ID.

[a]Facial features include bitemporal narrowing, narrow nasal bridge, deep/wide-set eyes.

[b]Hand or foot features include syndactyly, tapered, thin or hypoplastic digits, and arachnodactyly affecting either the hands and/or feet.

[c]Other organs include cardiac, genito-urinary, liver and eye.

[d]Behavioural concerns include anxiety, self-injury, hyperactivity and aggression.

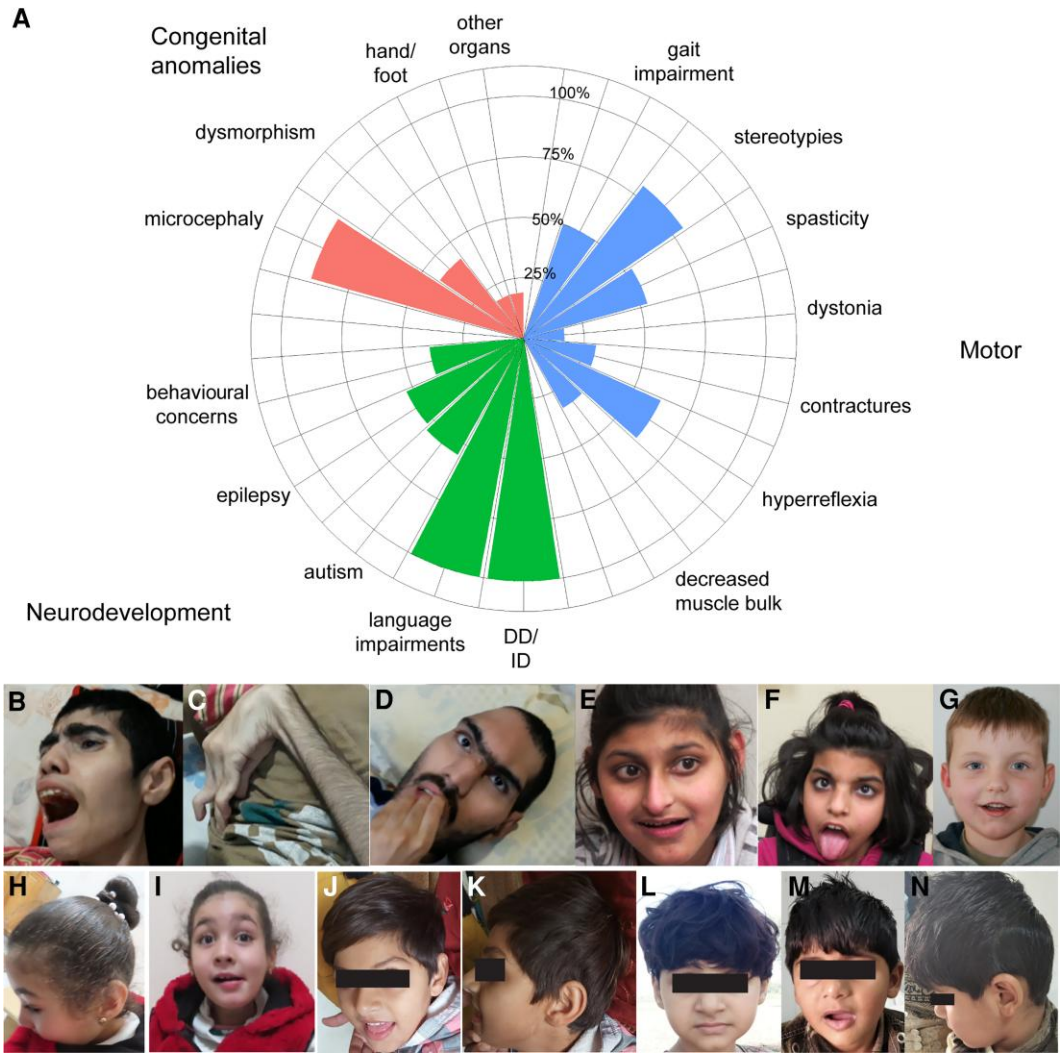

Figure 1 Clinical features of patients with TRAPPC6B variants. (**A**) Phenogram of frequency of phenotypic features for 29 new patients and 8 previously reported patients (Supplementary Table 1). Fields with missing data were not included in calculations for that feature. Behavioural phenotypes include aggression, self-injury, anxiety and hyperactivity. ID/DD = intellectual disability/developmental disability. (**B**–**N**) Photos of dysmorphic features. No unifying dysmorphic features were observed. (**B** and **C**) Patient 1 (Family 1) has gingival hypertrophy and swan neck deformity of fingers, representing dystonia. This patient also exhibited spastic-dystonic quadriplegia with contractures in the elbow flexors and plantar flexors, temporal wasting, muscle atrophy and curling of all her toes (not shown). (**D**) Patient 2 (Family 1) has synophrys, bitemporal narrowing, prominent cheekbones, a wide nasal root and bridge, and a papular lesion suspicious for an occult encephalocele. This patient also exhibited spastic-dystonic quadripledia, brachycephaly, trigonocephaly, temporal wasting and muscle atrophy in his proximal limb muscle (not shown). (**E**) Patient 5 (Family 4) has microcephaly, bitemporal narrowing, low anterior hairline, deep-set eyes, prominent ears, long nose with narrow nasal bridge and prognathia. (**F**) Patient 6 (Family 4) has microcephaly, bitemporal narrowing strabismus, positional plagiocephaly, deep set eyes, broad nasal root and narrow nasal bridge, and widely spaced teeth. (**G**) Patient 7 (Family 5) showing depressed nasal bridge, upturned nasal tip and thin upper lip. This patient also exhibited bilateral clinodactyly, tapered fingers and inverted nipples (not shown). (**H** and **I**) Patient 10 (Family 8) has microcephaly, long face, arched eyebrows, wide spaced eyes, almond shaped eye, straight nasal bridge, broad nose, broad chin and low set ears. Patient also exhibited arachnodactyly (not shown). (**J** and **K**) Patient 17 (Family 11) has narrow nasal bridge and posteriorly rotated ears. (**L**) Patient 18 (Family 11) has upslanting palpebral fissures and square nasal tip. (**M** and **N**) Patient 19 (Family 12) has microcephaly, bulbous nasal tip and creased earlobe.

matched large populations[29] did not identify a specific region driving the observed microcephaly (Fig. 2N). Of note, the individuals with missense variants (Patients 7 and 29) exhibited similar phenotypes, suggesting that missense variants could potentially impair protein function and disrupt nervous system development.

TRAPPC6B p.Q152* impairs TRAPPC3 binding, diminishing protein expression for TRAPPC6B and TRAPP II

Given that our previous work suggested that the carboxy-terminus of TRAPPC6A interacts with adaptor subunit TRAPPC2L and both TRAPPC6A and TRAPPC6B interact with TRAPPC2L and TRAPPC3,[10] we examined interactions between TRAPPC6B and both TRAPPC2L and TRAPPC3. While an interaction between both TRAPPC2L and TRAPPC3 was seen for the wild-type TRAPPC6B irrespective of the vectors used, only the TRAPPC3 interaction was affected by the p.Q152* allele from affected individuals in Family 15 (Fig. 3A and B).

This result suggests that the carboxy-terminus of TRAPPC6B is important for its interaction with TRAPPC3 and that this interaction is diminished in TRAPPC6B p.Q152*. Since the TRAPPC3-TRAPPC6B heterodimer is important for the assembly of the TRAPP complexes, it is not unreasonable to expect that

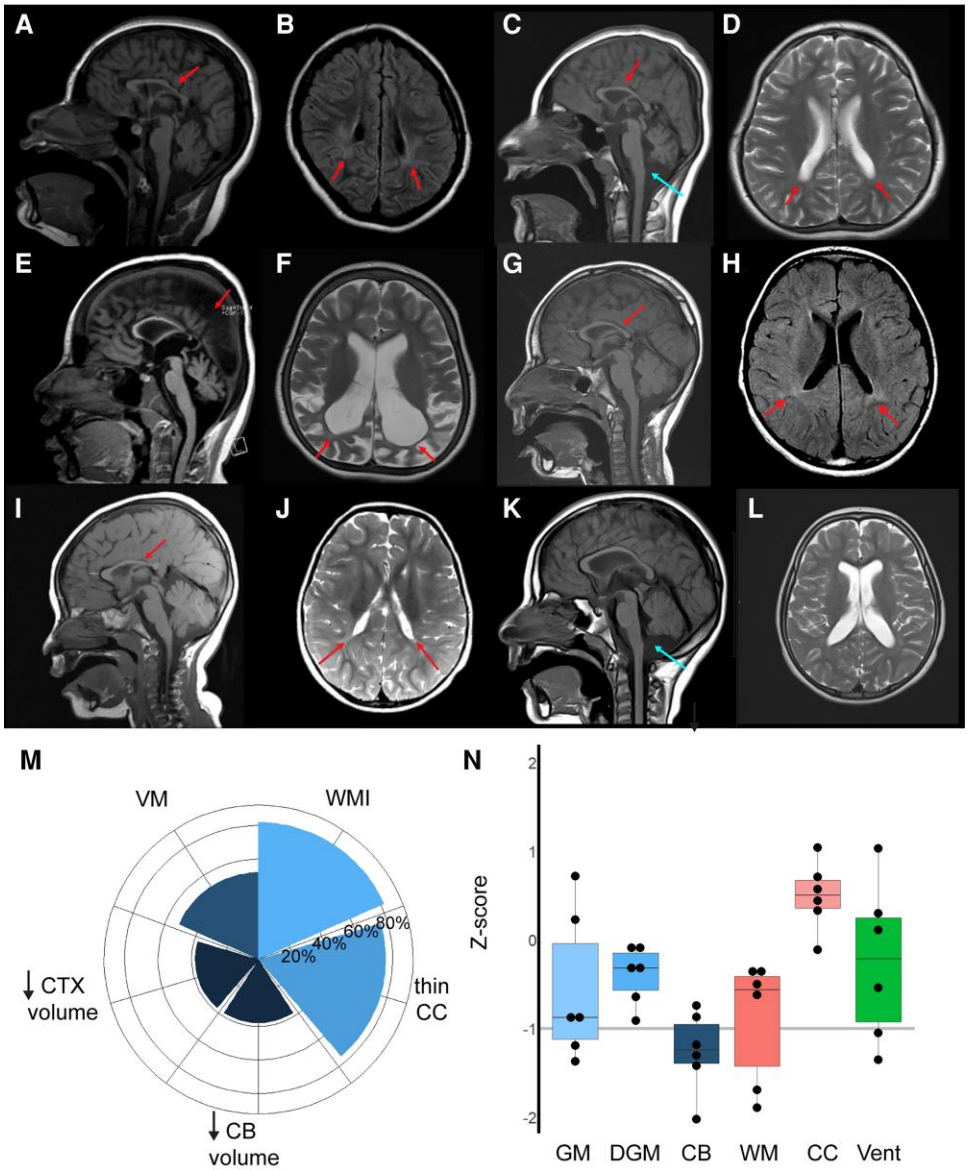

Figure 2 Qualitative and quantitative analysis of MRI images. (**A, C, E, G, I** and **K**) Sagittal MRI T1-weighted midline images. (**B** and **H**) Axial fluid attenuated inversion recovery (FLAIR) images. (**D, F, J** and **L**) Axial MRI T2-weighted images. (**A** and **B**) Patient 3, Family 2: 13-year-old female. (**A**) Small craniofacial ratio, thinning/foreshortening of the corpus callosum with greater involvement of the posterior fibres (red arrow). (**B**) Patchy FLAIR signal hyperintensity in the bilateral periventricular white matter (arrows) extending to the centrum semiovale, perirolandic and periatrial regions (not shown). (**C** and **D**) Patient 5, Family 4: 13-year-old female. (**C**) Small craniofacial ratio, diffuse thinning/foreshortening of the corpus callosum (red arrow) and brainstem and cerebellum volume loss (cyan arrow). (**D**) Abnormal angulation of the posterior margins of the ventricles (arrows). (**E** and **F**) Patient 6, Family 4: 9-year-old female. (**E**) Small craniofacial ratio, thinning/foreshortening of the corpus callosum and posterior greater than anterior parenchymal loss (arrow). (**F**) Diffuse parenchymal loss with preferential involvement of the posterior lobes, ex-vacuo dilatation and angulation of the ventricles (arrows). (**G** and **H**) Patient 13, Family 10: 6-year-old male. (**G**) Reduced frontal occipital diameter (FOD) and diffuse thinning and foreshortening of the corpus callosum (arrow). (**H**) Patchy FLAIR signal hyperintensity in periatrial white matter associated with abnormal square shape of the posterior margins of the lateral ventricles (arrows). (**I** and **J**) Patient 14, Family 10: 2-year-old female. (**I**) Reduced FOD, diffuse thinning and foreshortening of the corpus callosum (arrow). (**J**) Increased T2 signal in periatrial white matter associated with abnormal angulation of the posterior margins of the lateral ventricles (arrows). (**K** and **L**) Patient 16, Family 10: 5-year-old female. (**K**) Marginal FOD (red arrow) and inferior vermis hypoplasia (cyan arrow). (**L**) No signal abnormalities present. (**M**) Phenogram of MRI features for 16 new patients and 7 previously reported patients with MRI interpretation. Patient-specific details are provided in Supplementary Table 1. (**N**) Box and whisker plot of six structural measures quantified from brain MRI volumes of six patients, represented as z-scores in comparison to an age-matched control cohort of typically developing children. The threshold for significance of −1SD indicates reduced volume compared to the general population. Volume loss was identified in the cerebellum, but there was no consistent reduction in other measurements. Ventricle asymmetry measures laterality of ventricle expansion; no asymmetry was detected. Boxes represent 25th and 75th percentiles with median line; whiskers represent data range. CB = cerebellum; CC = corpus callosum; CTX = cortex; DGM = deep grey matter; GM = grey matter; Vent = ventricle asymmetry; VM = ventriculomegaly; WM = white matter; WMI = white matter hyperintensity or abnormalities.

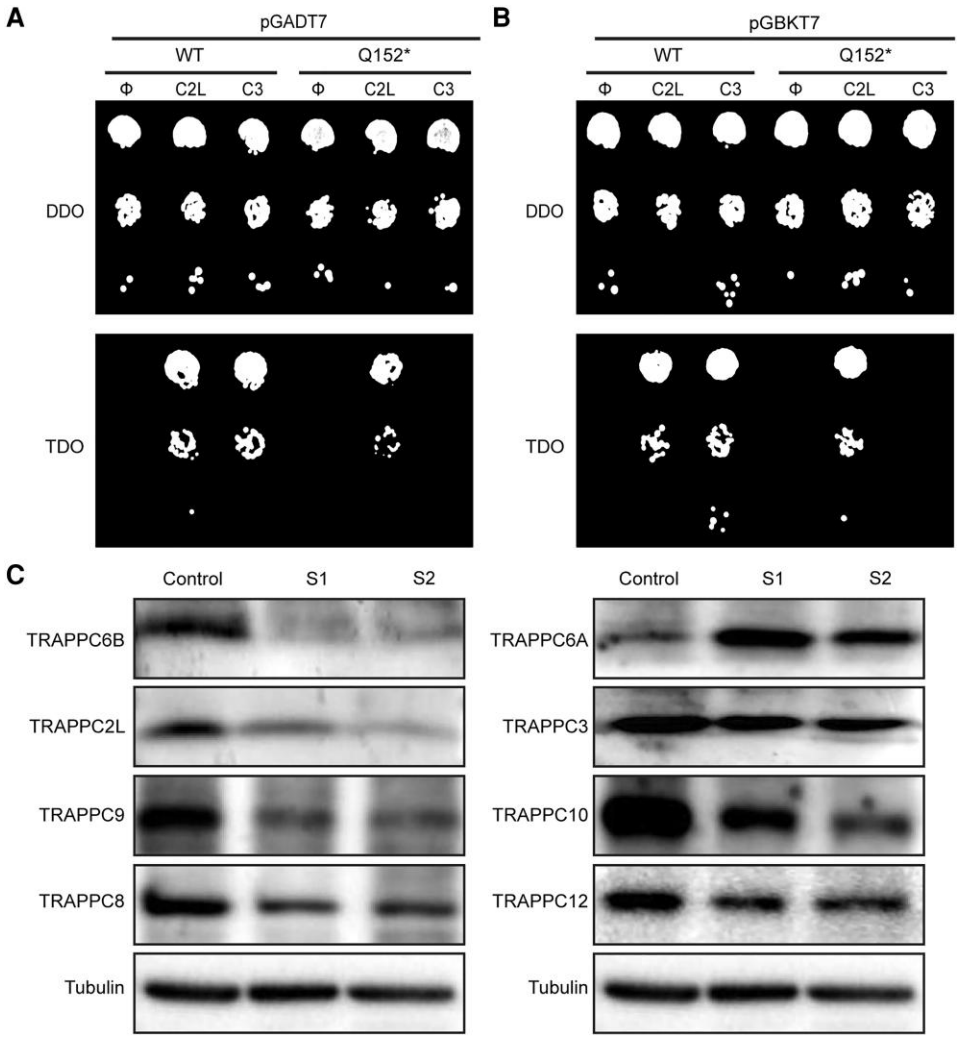

Figure 3 TRAPPC6B variants affect the stability of TRAPP II. TRAPPC6B (wild-type or p.Q152* variant) was cloned into either pGADT7 (**A**) or pGBKT7 (**B**); TRAPPC2L and TRAPPC3 were cloned into either pGBKT7 (**A**) or pGADT7 (**B**) and transformed into haploid yeast cells. In some cases, an empty vector (Φ) was used. The cells were mated, diploids selected and then spotted as serial dilutions on plates lacking leucine and tryptophan (DDO) or plates lacking leucine, tryptophan and histidine (TDO). (**C**) Fibroblasts from control or affected individuals from Family 15 (p.Q152*) were lysed and probed for the indicated TRAPP proteins or for tubulin as a loading control. WT = wild-type.

TRAPPC6B variants will decrease the presence of subunits that rely on this heterodimer to associate with TRAPP complexes. Indeed, in p.Q152* fibroblasts, several TRAPP protein levels were decreased, with the strongest effect seen for the two TRAPP II-specific proteins TRAPPC10 and TRAPPC9 (Fig. 3C). There was a near complete absence of detectable amounts of TRAPPC6B, suggesting potential nonsense mediated decay or truncated protein instability (Fig. 3C). It is noteworthy that we consistently saw an increase in the levels of TRAPPC6A in the fibroblasts from the affected individuals, perhaps representing an attempted compensatory response.

TRAPP II complex members associate preferentially with TRAPPC6B

We next examined whether TRAPPC6B was preferentially associated with TRAPP II complexes. To perform this experiment, HeLa cells were mock transfected or co-transfected with TRAPPC6A-V5/TRAPPC10-FLAG, TRAPPC6A-V5/TRAPPC11-FLAG, TRAPPC6B-V5/TRAPPC10-FLAG or TRAPPC6B-V5/TRAPPC11 and associated proteins were collected on beads harbouring anti-FLAG IgG and probed for V5 and FLAG. TRAPPC11 transfections target TRAPP III, while the TRAPPC10 transfections target TRAPP II.

Unlike TRAPPC6A, which equally co-precipitated with TRAPPC10 and TRAPPC11, TRAPPC6B was significantly more enriched with TRAPPC10 compared to TRAPPC11 (Fig. 4A and B). These results suggest that TRAPP II complexes are enriched in TRAPPC6B compared to TRAPP III.

Patient-derived fibroblasts have ER-Golgi trafficking defects and altered Golgi morphology

Previous studies have shown an anterograde trafficking defect for variants in most TRAPP-associated genes.[8,10,14,18] Therefore, we subjected fibroblasts derived from Families 4 (c.149+2 T>A splice-site; Patients 5 and 6) and 15 (p.Q152*; Patients 23 and 24) to a membrane trafficking assay.[30] In all four cases, upon biotin-mediated release of an ER-retained protein there was a delay in transport to the Golgi compared to control (Fig. 5A and B). This was determined to be TRAPPC6B-related since transfection of RFP-tagged TRAPPC6B resulted in a noticeable rescue of this trafficking defect. Golgi fragmentation is also commonly seen in cells

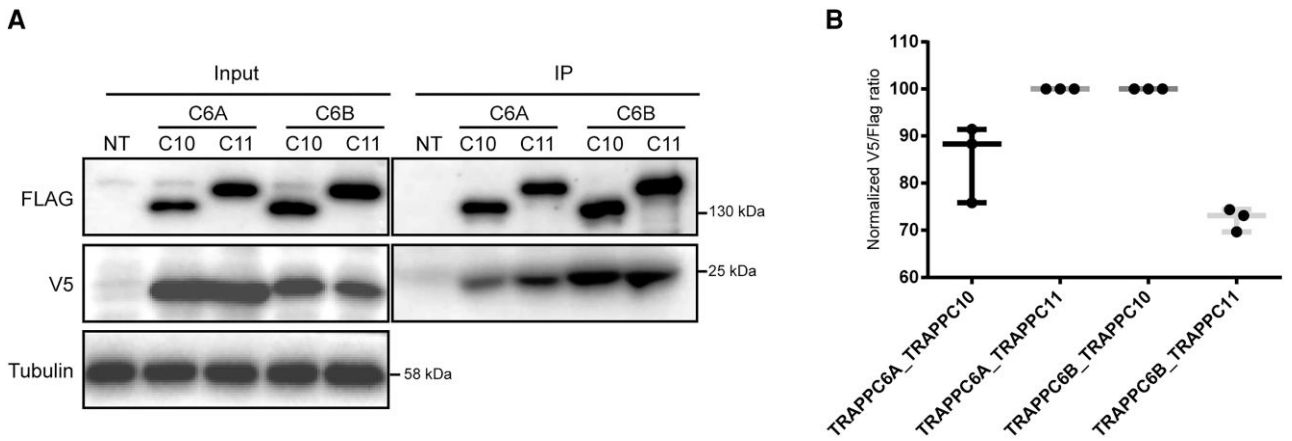

Figure 4 TRAPPC6B preferentially associates with the TRAPP II complex. (**A**) HeLa cells were either untransfected (NT) or co-transfected with TRAPPC6A-V5/TRAPPC10-FLAG, TRAPPC6A-V5/TRAPPC11-FLAG, TRAPPC6B-V5/TRAPPC10-FLAG or TRAPPC6B-V5/TRAPPC11. After 48 h, the cells were lysed and treated with anti-FLAG IgG agarose beads. The eluates from the immunoprecipitation were probed for V5, FLAG and tubulin. The blot is representative of at least three biological replicates. Inputs represent 10% of the sample subjected to immunoprecipitation (IP). (**B**) Quantification of the ratio of V5 immunoprecipitated with FLAG from three different experiments. The integrated density of V5, FLAG and background nearby for each band was measured using ImageJ v1.53. To obtain the corrected integrated density, the background value for each band was subtracted. The V5/FLAG ratio was then calculated using the corrected integrated densities and normalized to the highest signal detected for FLAG.

harbouring TRAPP gene mutations as well as in cells with mutations in other membrane trafficking-related proteins.[35] When the fibroblasts from affected individuals were compared to control, a significant increase in Golgi fragmentation was seen (Fig. 5C and D). This increase was rescued to near wild-type levels by transfection of wild-type TRAPPC6B. Together, our functional studies suggest that variants in TRAPPC6B can disrupt ER to Golgi protein trafficking and lead to altered Golgi morphology.

Loss of neuronal TRAPPC6B impairs locomotion and wing posture in *Drosophila*

We examined whether TRAPPC6B could regulate neuromotor function in a *Drosophila* model. The *Drosophila* orthologue, Trs33, has excellent conservation with TRAPPC6B (DRSC integrated orthologue prediction tool score = 15/15) with 72% similarity and 54% identity (flyrnai.org). As *Trs33* is an essential gene for development, we used an RNAi knockdown approach specifically in neurons under the ELAV-Gal4 driver. Neuronal expression of Trs33 shRNA decreased distance traveled in a locomotor assay compared to the heterozygous controls of the Gal4 and UAS lines alone (Fig. 6A). Additionally, an abnormality of wing posture was noted in 10.6% of these animals, suggesting defects in the innervation of the indirect flight muscles (Fig. 6B). Together, this suggests TRAPPC6B is crucial for motor function.

Discussion

Marin-Valencia *et al.*[9] recently reported a founder *TRAPPC6B* homozygous splice-site variant segregating with disease in three Egyptian families and found that morpholino treatment against *Danio* TrappC6B led to reduced head size and increased spontaneous neuronal activity in zebrafish. We present here 29 individuals from 18 families with biallelic variants in *TRAPPC6B*. These individuals share a syndromic phenotype consisting of primary microcephaly, global developmental delay/intellectual disability, stereotypies and impaired expressive language. Brain MRI findings include volume loss, thin corpus callosum and white matter signal abnormalities. Variable features include epilepsy, spasticity/dystonia and dysmorphic features. Our findings thus provide an independent validation for biallelic *TRAPPC6B* variants as a cause of a complex neurodevelopmental disorder and expand on the clinical features.

Notably, two individuals in our series harboured *TRAPPC6B* variants of unknown significance (Patients 7 and 29). The individual with compound heterozygous splice and small deletion variants (Patient 7) had a milder phenotype, gaining the ability to use limited expressive language, falling short of a formal diagnosis of microcephaly and achieving independent walking by age 3. The homozygous missense variant (p.G124V) has a CADD score of 32, is absent from gnomAD and classified as a variant of uncertain significance (VOUS) in VarSome. This individual (Patient 29) has clinical features that match the remaining cohort, including microcephaly, spasticity, epilepsy and a thin corpus callosum. However, we were not able to conduct functional studies on this variant. This suggests that missense variants can contribute to a *TRAPPC6B* genetic disorder, with similar but potentially milder manifestations, but further studies are needed. The remaining 27 individuals in the present cohort and those reported by Marin-Valencia *et al.*[9] all had homozygous splice-site and early stop variants. We confirmed diminished protein expression in a family with a homozygous early stop variant (p.Q152*), consistent with a loss-of-function variant that may manifest with decreased protein abundance or the loss of an as-yet unidentified motif in the carboxy-terminus important for subcellular localization or protein-protein interactions. One limitation of this work is the fact that we only tested the effect of this particular variant on TRAPPC6B levels.

Our biochemical studies suggest that variants in TRAPPC6B such as p.Q152* likely impair TRAPP II complex stability by a weakened interaction with TRAPPC3 and decreasing protein expression for TRAPPC6B and TRAPP II complex members. TRAPPC6B appears to associate preferentially with TRAPP II compared to TRAPP III. It is interesting that TRAPPC6A levels increase in the absence of TRAPPC6B as seen in affected individuals of Family 15. It is possible that TRAPPC6A can partially compensate for the loss of TRAPPC6B. This would be consistent with the studies of TRAPP GEF activity towards Rab for recombinant *Drosophila* and human complexes.[3,36]

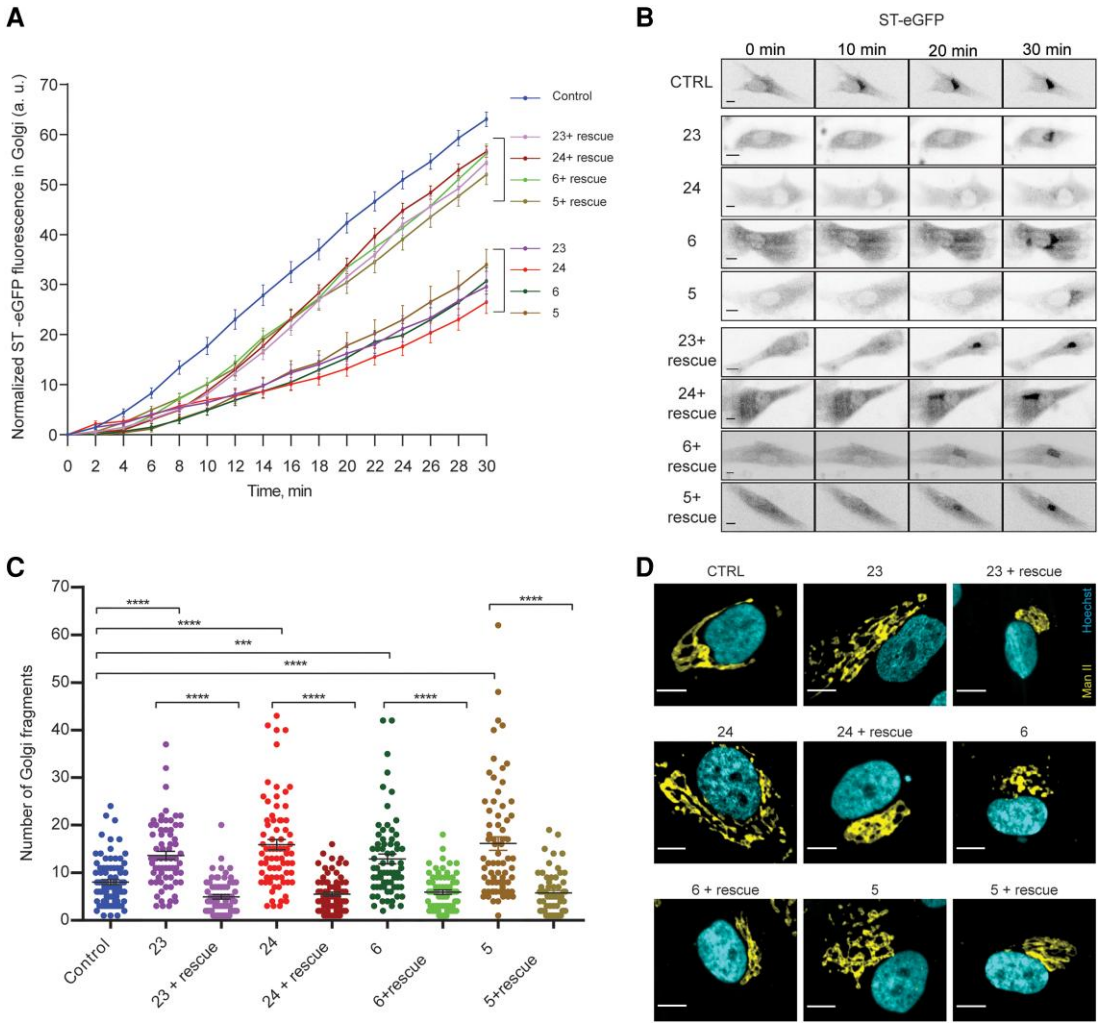

Figure 5 Fibroblasts from individuals with TRAPPC6B variants display membrane trafficking defects and have fragmented Golgi. (**A**) Fibroblasts from Families 4 (c.149+2 T>A splice-site; Patients 5 and 6) and 15 (p.Q152*; Patients 23 and 24) were transfected with sialyl transferase (ST-GFP) and incubated overnight. The next day, cells were treated with 60 µM biotin and imaged every 2 min. Golgi-associated fluorescence was quantified and plotted as a function of time. In some cases, TRAPPC6B-RFP was co-transfected to verify a rescue of the trafficking defect. The error bars represent the standard error of the mean (SEM) at each time point. (**B**) Representative images used for quantification of the retention using selective hooks trafficking assay at 0, 10, 20 and 30 min. *n*-values ranged from 48 to 61 and come from at least three biological replicates. Scale bar = 10 µm. (**C**) Fibroblasts were either untransfected or transfected with TRAPPC6B-RFP, fixed and stained for mannosidase II as a Golgi marker. The mannosidase II-positive structures were quantified as described in the methods section. Bars represent SEM. *n*-values ranged from 65 to 82 and come from at least three biological replicates. (**D**) Representative images used for the quantifying the number of Golgi fragments. Scale bar = 10 µm. CTRL = control.

In *Drosophila*, only a single (TRAPPC6B) homologue is found, while humans have both TRAPPC6A and TRAPPC6B. Therefore, *Drosophila* TRAPP complexes do not distinguish between the two TRAPPC6 human orthologues and TRAPP III is functional with TRAPPC6B. In the human recombinant complexes, TRAPPC6A was used for assembling both TRAPP II and III, and both complexes were functional.[3,36] It remains possible that had TRAPPC6B been used in the recombinant TRAPP II complex, stronger or additional GEF activity would have been seen. Nevertheless, our present study suggests a bias for TRAPPC6B in TRAPP II and implies the cell has a mechanism to distinguish and incorporate specific TRAPPC6 orthologues into specific TRAPP complexes. It is presently unclear how this would be accomplished.

Disruption of TRAPP II stability has been shown previously to affect anterograde trafficking.[18] Biallelic variants of *TRAPPC6B* show similar cellular features, such as an ER-to-Golgi trafficking defect and altered Golgi morphology.

We found that neuronal loss of TRAPPC6B in a *Drosophila* model impaired locomotion and wing posture. The erect wing phenotype has been linked to impaired synaptic growth[37] and disrupted CNS commissures and longitudinal tracts innervating the indirect flight muscles which regulate wing posture.[38] Knocking down Trs33 in *Drosophila* with the Mef2 muscle and neuron expressing Gal4-driver was reported to impair flight ability but without obvious changes to the flight muscles, myofibrils or sarcomeres themselves.[39] Together with our ELAV-mediated neuronal knockdown, this suggests a neuronal origin for the previously reported flight muscle weakness that has similarities to the postural/locomotor impairments in *TRAPPC6B*-affected individuals.

TRAPPC6B-associated phenotypes overlap substantially with variants in genes encoding other TRAPP subunits. These phenotypes include intellectual disability, movement disorders, white matter involvement, cerebellar volume loss, microcephaly and

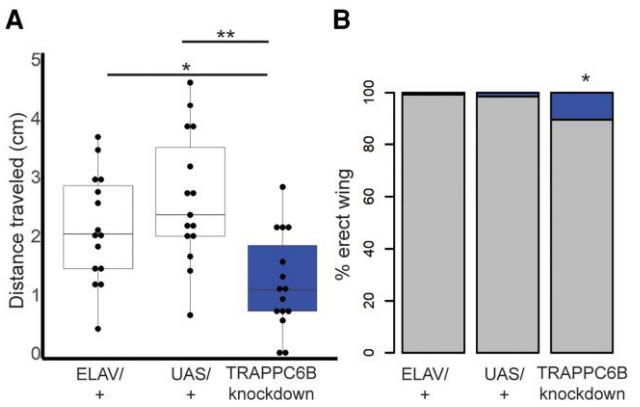

Figure 6 Neuronal TRAPPC6B knockdown impairments in a *Drosophila* model. (**A**) Box and whisker plot of distance travelled in 3 s in negative geotaxis assay comparing Gal4 and UAS driver heterozygotes and shRNA neuronal-driven expression for TRAPPC6B knockdown. Statistics determined using paired *t*-test ($n = 16$ trials). Boxes represent 25th and 75th percentiles with median line; whiskers represent range of data. *$P < 0.01$, *$P < 0.001$. (**B**) Erect wing phenotype is significantly increased in TRAPPC6B knockdown compared to heterozygous controls. ($n = 113$–137 flies/genotype). Statistics determined both three-way and pairwise against individual controls using chi-squared analysis. *$P < 0.01$.

muscle involvement (Table 1).[8] Many TRAPP-related disorders, particularly those affecting TRAPP III, identified a progressive loss of cerebral volume over time (Table 1). However, we did not find evidence that loss of *TRAPPC6B* function causes neurodegeneration. Treating clinicians did not note progressive microcephaly and available occipital frontal circumference measurements seem to start low at birth and maintain the same course. Consistent with the biochemical studies, we found *TRAPPC6B* phenotypes overlapped more closely for genes exclusively localized to TRAPP II [*TRAPPC9* (#613192) and *TRAPPC10* (*602103)]. In contrast, individuals with variants in genes exclusively encoding autophagy-associated TRAPP III components (*TRAPPC11* and *TRAPPC12*) are notably different from the *TRAPPC6B* patients. *TRAPPC11* variants lead to a complex neurodevelopmental disorder with muscular dystrophy and visual system impairments and individuals with *TRAPPC12* display a progressive encephalopathy. This supports the conclusion that *TRAPPC6B* is important for TRAPP II complex function with impairments resulting in a distinct and recognizable TRAPPopathy. A major challenge in understanding the neurological disorder linked to TRAPPII variants is the consequence of trafficking defects on neuronal function. We identified a potential defect in neuronal innervation in the fly model; however, we were unable to investigate further due to the lack of human neuronal cells. Cellular reprograming of patient fibroblasts into patient-derived induced pluripotent stem cells that can be induced to differentiate into specific neuronal cells can overcome this limitation and provide better insight into the aetiology of neurodevelopmental disorders associated with TRAPPII variants.

Data availability

The authors confirm that the data supporting the findings of this study are available within the article and/or its Supplementary material. Additional raw and/or de-identified data supporting the findings of this study are available from the corresponding authors upon reasonable request.

Acknowledgements

We are grateful to the patients and their families for involvement in these studies. We acknowledge Dr. Hossein Mozhdehipanah and Dr. Paulien A. Terhal for providing patient clinical information. We appreciate the assistance of Dr. Bob Argiropoulos and Nadine Gamache with fibroblast cultures.

Funding

Portions of this work were supported by a Cerebral Palsy Alliance Research Foundation Career Development Award (CDG01318) to S.B. and by the US National Institute of Neurological Disorders and Stroke (1R01NS106298 and 1R01NS127108 to M.C.K.).

Competing interests

The authors report no competing interests.

Supplementary material

Supplementary material is available at *Brain* online.

References

1. Chin HF, Cai Y, Menon S, Ferro-Novick S, Reinisch KM, De La Cruz EM. Kinetic analysis of the guanine nucleotide exchange activity of TRAPP, a multimeric Ypt1p exchange factor. *J Mol Biol*. 2009;389:275-288.
2. Riedel F, Galindo A, Muschalik N, Munro S. The two TRAPP complexes of metazoans have distinct roles and act on different Rab GTPases. *J Cell Biol*. 2018;217:601-617.
3. Jenkins ML, Harris NJ, Dalwadi U, *et al*. The substrate specificity of the human TRAPPII complex's Rab-guanine nucleotide exchange factor activity. *Commun Biol*. 2020;3:735.
4. Knödler A, Feng S, Zhang J, *et al*. Coordination of Rab8 and Rab11 in primary ciliogenesis. *Proc Natl Acad Sci U S A*. 2010; 107:6346-6351.
5. Westlake CJ, Baye LM, Nachury MV, *et al*. Primary cilia membrane assembly is initiated by Rab11 and transport protein particle II (TRAPPII) complex-dependent trafficking of Rabin8 to the centrosome. *Proc Natl Acad Sci U S A*. 2011;108:2759-2764.
6. Scrivens PJ, Noueihed B, Shahrzad N, Hul S, Brunet S, Sacher M. C4orf41 and TTC-15 are mammalian TRAPP components with a role at an early stage in ER-to-Golgi trafficking. *Mol Biol Cell*. 2011; 22:2083-2093.
7. Stanga D, Zhao Q, Milev MP, Saint-Dic D, Jimenez-Mallebrera C, Sacher M. TRAPPC11 Functions in autophagy by recruiting ATG2B-WIPI4/WDR45 to preautophagosomal membranes. *Traffic*. 2019;20:325-345.
8. Sacher M, Shahrzad N, Kamel H, Milev MP. TRAPPopathies: An emerging set of disorders linked to variations in the genes encoding transport protein particle (TRAPP)-associated proteins. *Traffic*. 2019;20:5-26.
9. Marin-Valencia I, Novarino G, Johansen A, *et al*. A homozygous founder mutation in TRAPPC6B associates with a neurodevelopmental disorder characterised by microcephaly, epilepsy and autistic features. *J Med Genet*. 2018;55(1):48–54.
10. Al-Deri N, Okur V, Ahimaz P, *et al*. A novel homozygous variant in TRAPPC2L results in a neurodevelopmental disorder and disrupts TRAPP complex function. *J Med Genet*. 2021;58(9): 592–601.
11. Milev MP, Graziano C, Karall D, *et al*. Bi-allelic mutations in TRAPPC2L result in a neurodevelopmental disorder and have

an impact on RAB11 in fibroblasts. *J Med Genet*. 2018;55(11): 753–764.
12. Saad AK, Marafi D, Mitani T, *et al*. Biallelic in-frame deletion in TRAPPC4 in a family with developmental delay and cerebellar atrophy. *Brain*. 2020;143:e83.
13. Ghosh SG, Scala M, Beetz C, *et al*. A relatively common homozygous TRAPPC4 splicing variant is associated with an early-infantile neurodegenerative syndrome. *Eur J Hum Genet*. 2021;29:271-279.
14. Van Bergen NJ, Guo Y, Al-Deri N, *et al*. Deficiencies in vesicular transport mediated by TRAPPC4 are associated with severe syndromic intellectual disability. *Brain*. 2020;143(3):112–130.
15. Mohamoud HS, Ahmed S, Jelani M, *et al*. A missense mutation in TRAPPC6A leads to build-up of the protein, in patients with a neurodevelopmental syndrome and dysmorphic features. *Sci Rep*. 2018;8:2053.
16. Bodnar B, DeGruttola A, Zhu Y, *et al*. Emerging role of NIK/IKK2-binding protein (NIBP)/trafficking protein particle complex 9 (TRAPPC9) in nervous system diseases. *Transl Res*. 2020; 224:55-70.
17. Kakar N, Goebel I, Daud S, *et al*. A homozygous splice site mutation in TRAPPC9 causes intellectual disability and microcephaly. *Eur J Med Genet*. 2012;55:727-731.
18. Rawlins LE, Almousa H, Khan S, *et al*. Biallelic variants in TRAPPC10 cause a microcephalic TRAPPopathy disorder in humans and mice. *PLoS Genet*. 2022;18:e1010114.
19. Santos-Cortez RLP, Khan V, Khan FS, *et al*. Novel candidate genes and variants underlying autosomal recessive neurodevelopmental disorders with intellectual disability. *Hum Genet*. 2018;137:735-752.
20. Wang X, Wu Y, Cui Y, Wang N, Folkersen L, Wang Y. Novel TRAPPC11 mutations in a Chinese pedigree of limb girdle muscular dystrophy. *Case Rep Genet* 2018; 2018:8090797.
21. Milev MP, Grout ME, Saint-Dic D, *et al*. Mutations in TRAPPC12 manifest in progressive childhood encephalopathy and Golgi dysfunction. *Am J Hum Genet*. 2017;101:291-299.
22. Bassik MC, Kampmann M, Lebbink RJ, *et al*. A systematic mammalian genetic interaction map reveals pathways underlying ricin susceptibility. *Cell*. 2013;152:909-922.
23. Scrivens PJ, Shahrzad N, Moores A, Morin A, Brunet S, Sacher M. TRAPPC2L Is a novel, highly conserved TRAPP-interacting protein. *Traffic*. 2009;10:724-736.
24. Kümmel D, Müller JJ, Roske Y, Henke N, Heinemann U. Structure of the Bet3-Tpc6B core of TRAPP: Two tpc6 paralogs form trimeric complexes with Bet3 and Mum2. *J Mol Biol*. 2006;361:22-32.
25. Kümmel D, Oeckinghaus A, Wang C, Krappmann D, Heinemann U. Distinct isocomplexes of the TRAPP trafficking factor coexist inside human cells. *FEBS Lett*. 2008;582:3729-3733.
26. Tokarev AA, Taussig D, Sundaram G, *et al*. TRAPP II complex assembly requires Trs33 or Trs65. *Traffic*. 2009;10(12):1831–1844.
27. Harripaul R, Vasli N, Mikhailov A, *et al*. Mapping autosomal recessive intellectual disability: Combined microarray and exome sequencing identifies 26 novel candidate genes in 192 consanguineous families. *Mol Psychiatry*. 2018;23:973-984.
28. Nair P, El-Bazzal L, Mansour H, *et al*. Further delineation of the TRAPPC6B disorder: Report on a new family and review. *J Pediatr Genet*. 2019;8:252-256.
29. Pagnozzi AM, Dowson N, Doecke J, *et al*. Identifying relevant biomarkers of brain injury from structural MRI: Validation using automated approaches in children with unilateral cerebral palsy. *PLoS One*. 2017;12:e0181605.
30. Boncompain G, Divoux S, Gareil N, *et al*. Synchronization of secretory protein traffic in populations of cells. *Nat Methods*. 2012; 9:493-498.
31. Milev MP, Hasaj B, Saint-Dic D, Snounou S, Zhao Q, Sacher M. TRAMM/Trappc12 plays a role in chromosome congression, kinetochore stability, and CENP-E recruitment. *J Cell Biol*. 2015;209:221-234.
32. Ke H, Feng Z, Liu M, *et al*. Collagen secretion screening in Drosophila supports a common secretory machinery and multiple rab requirements. *J Genet Genomics*. 2018;45:299-313.
33. Kim M, Sandford E, Gatica D, *et al*. Mutation in ATG5 reduces autophagy and leads to ataxia with developmental delay. *Elife*. 2016;5:e12245.
34. Fernandes C, Rao Y. Genome-wide screen for modifiers of Parkinson's disease genes in Drosophila. *Mol Brain*. 2011;4:17.
35. Makhoul C, Gosavi P, Gleeson PA. Golgi Dynamics: The morphology of the mammalian Golgi apparatus in health and disease. *Front Cell Dev Biol*. 2019;7:112.
36. Harris NJ, Jenkins ML, Dalwadi U, *et al*. Biochemical insight into novel Rab-GEF activity of the mammalian TRAPPIII Complex. *J Mol Biol*. 2021;433:167145.
37. Haussmann IU, White K, Soller M. Erect wing regulates synaptic growth in Drosophila by integration of multiple signaling pathways. *Genome Biol*. 2008;9:R73.
38. DeSimone S, Coelho C, Roy S, VijayRaghavan K, White K. ERECT WING, the Drosophila member of a family of DNA binding proteins is required in imaginal myoblasts for flight muscle development. *Development*. 1996;122:31-39.
39. Schnorrer F, Schönbauer C, Langer CC, *et al*. Systematic genetic analysis of muscle morphogenesis and function in Drosophila. *Nature*. 2010;464:287-291.